Virginia Tech Aerospace Engineering
Spring Semester Final Report
5 May, 2004

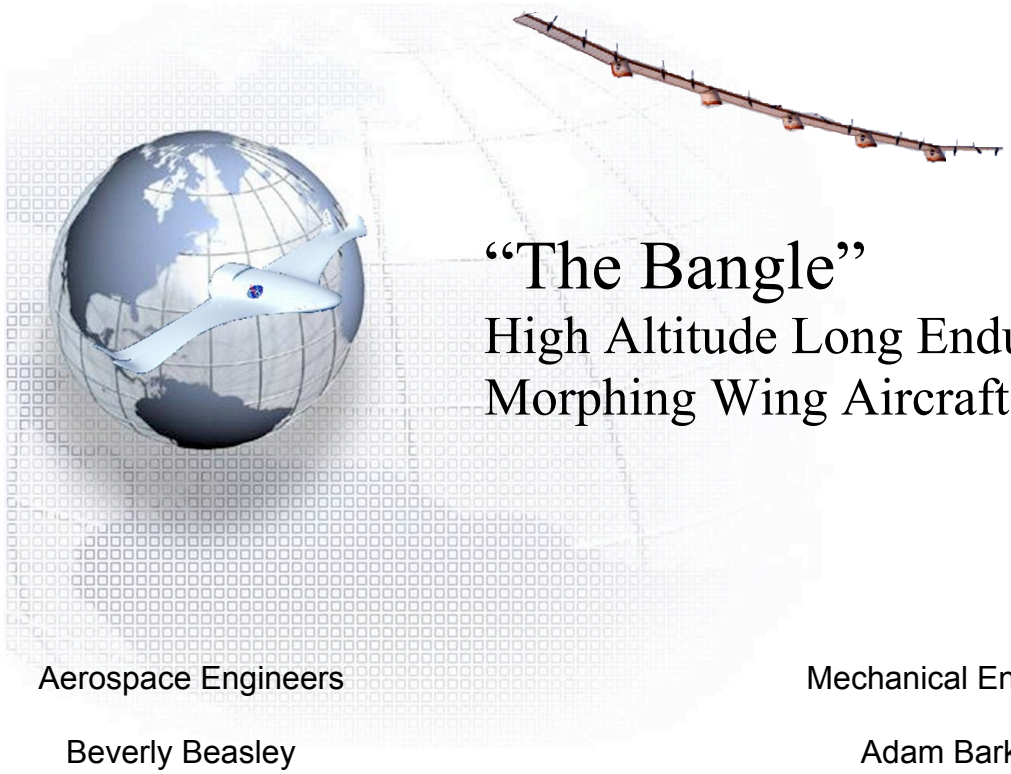

"The Bangle"
High Altitude Long Endurance Morphing Wing Aircraft

Aerospace Engineers

Beverly Beasley
David Pfeffer
Daniel Pedraza
James Pembridge

Mechanical Engineers

Adam Barker
Justin Farmer
Jonathan Inman
Peyton Martin
Christopher Minton
Josiah Oliver

CIMSS

Virginia Tech
VIRGINIA POLYTECHNIC INSTITUTE AND STATE UNIVERSITY

aerospace & ocean engineering

Contents

List of Figures

1 Introduction

1.1 Definition of HALE aircraft

The Acronym HALE characterizes High Altitude Long Endurance aircraft that have extremely high range and endurance capabilities when compared to conventional aircraft. HALE aircraft are being implemented to perform very long-endurance, high-altitude environmental science, surveillance, and commercial telecommunications relay missions. Due to the hostile low pressure, low Reynolds number environment in the upper atmosphere, HALE aircraft are being designed as Unmanned Aerial Vehicles (UAV).

1.2 History of HALE

HALE aircraft have been considered as a cheaper alternative to satellites for atmospheric research, earth and weather observation, and particularly communications since the late 1950s. A decade later, new attention was focused on aircraft propelled by solar power. Solar power photovoltaic (PV) cells, are not very efficient, and the amount of energy provided by the Sun over a unit area is relatively modest. This means that a solar powered aircraft must be built light-weight to allow low-powered electric motors to propel it.

In the early 1970's, a NASA engineer named Dale Reed was investigating how to sample the atmosphere at very high altitudes, up to 70,000 feet (21 kilometers). To aid in this investigation, NASA work on high-altitude UAVs was revived in the late 1980s, leading to the ERAST program in 1987 and 1988. NASA's Environmental Research Aircraft and Sensor Technology (ERAST) program conducted atmospheric ozone-layer

depletion studies using two piloted NASA aircraft. Operating over Antarctica however, where ozone depletion took place, was regarded as risky, since the pilot would not likely survive if a bale out was necessary. This led to efforts of continuing these studies using unmanned aircraft. (NASA, Dryden)

1.3 Comparator Aircraft

In the VT HALE design process, HALE aircraft were researched in order to recreate a morphing HALE aircraft with comparable flying characteristics of full-scale HALE aircraft built today. Some comparator aircraft were Centurion, Global Hawk, and HELIOS.

1.3.1 Centurion

Centurion is a lightweight, solar-powered, remotely piloted flying wing aircraft that demonstrates the technology of applying solar power for long-duration, high-altitude flight. It is considered to be a prototype technology demonstrator for a future fleet of solar-powered aircraft that could stay airborne for weeks or months on different scientific sampling or imaging missions. Centurion was built by AeroVironment, which finished the Centurion in the summer of 1998. The UAV made its first flight in November 1998. It had a span of 206 feet (62.8 meters), and weighed 1,385 pounds (630 kilograms). The expected ceiling for Centurion was 100,000 feet (30,500 meters). The Centurion prototype was then developed further to act as a prototype for another of our comparator aircraft: Helios.

1.3.2 HELIOS

The HELIOS Prototype was a unique electrically powered experimental lightweight flying wing developed by AeroVironment, under NASA's Environmental

Research Aircraft and Sensor Technology (ERAST) program. Using energy derived from the sun by day and from fuel cells at night, HELIOS was designed as the forerunner of high-altitude unmanned aerial vehicles. The two primary goals of the HELIOS Prototype development were to demonstrate sustained flight at an altitude near 100,000 feet and flying non-stop for at least 24 hours, including at least 14 hours above 50,000 feet. HELIOS is the largest of the comparator aircraft with a wingspan of 247 feet and a gross weight of 2048 pounds. HELIOS achieved a record altitude of 96,863 feet on an almost 17-hour flight on August 13, 2001.

1.3.3 Global Hawk

Global Hawk was conceived in 1995 by DARPA and Northrop Grumman as a long-endurance, unmanned airborne reconnaissance platform. Its primary objective is to provide military field commanders with high resolution and near-real-time imagery of large geographic areas. Global Hawk is capable of flying 1200 nautical miles to an area of interest, stay in the air for 24 hours and fly back to its operating base. It is somewhat of an outlier HALE aircraft as the Reynolds number, lift coefficient, and wing loading are out of the range of the other comparator aircraft in this study. Global Hawk has a wingspan that is about half the size of other HALE aircraft, measuring only 116.2 feet. Its gross takeoff weight is 25,600 lbs, much heavier than the other comparator aircraft. Global Hawk is also unique in that it was designed as a totally autonomous system. It is not controlled by a ground-based pilot using conventional controls, but rather is controlled by mouse clicks on a workstation controlled by the Command and Control Operator (CCO).

1.4 Control authority problems with HALE aircraft

Due to the extremely long wingspan and flexible body of most HALE aircraft, roll control is a problem. This issue is significant during takeoff and landing where quick control response is a necessity for safe operation. To counteract this problem, most HALE aircraft must wait for near perfect weather conditions with little wind and no gusts to assure a safe departures and landings.

HALE aircraft perform well at upper altitudes, but are not capable of matching that performance at lower altitudes. It is important to note that HELIOS was destroyed after it experienced control problems about a half-hour after takeoff on a checkout flight and "suffered some structural failures after entering a series of severe pitch oscillations." The VT Morphing Wing Team plans to improve on the HALE aircraft designs through morphing to increase performance in both flight regimes.

2 Request for Proposal

Virginia Tech's Morphing Wing Team intended to address control issues with current HALE aircraft using morphing technology. The project was driven by a NASA grant given to fabricate a scale HALE aircraft that would demonstrate control authority at takeoff and landing through morphing.

2.1 Project Goals

The goal of the project was to build and flight test a $1/16^{th}$ scale model of a HALE aircraft that was aerodynamically similar to current HALE aircraft and provided sufficient control authority for takeoff and landing in less than perfect conditions.

The aircraft was to exhibit morphing technology that would increase the wingspan 300% for cruise. The short wingspan would assure roll control in gusty winds, and the increased wingspan would be used for climb and cruise.

To aerodynamically model HALE aircraft, the model had to fly at a Reynolds number, lift coefficient, and wing loading similar to current HALE aircraft. Matching the aerodynamic properties drove the sizing of the model.

To mechanically model full-scale HALE aircraft, the wing extension system was to be designed in a fashion that was easily replicated on a large scale. The model was to use a simplistic design to extend the wings smoothly and symmetrically.

3 Aerodynamic similarity to current HALE aircraft

Experimental data for scale-model aircraft are used to define the aerodynamic characteristics of full-scale aircraft. To apply the data to a full-scale aircraft, the scale model must be aerodynamically equivalent to its full-scale design. This aerodynamic similarity permits the data collected during flight testing to be directly applied to a full-scale aircraft.

Typical HALE aircraft fly between 60,000 feet and 100,000 feet. The VT $1/16^{th}$ scale model will be flight tested at 2,000 feet. In order to model the aerodynamic performance of a HALE aircraft at altitude, the flight Reynolds number, lift coefficient, and wing loading had to be in the same range of current HALE aircraft.

3.1 Lift Coefficient

The lift coefficient, C_L is defined as:

$$C_L = \frac{L}{\frac{1}{2}\rho V^2 S}$$

where L is the lift produced, _ is the density, V is the velocity, and S is the **p**lanform area.

Most HALE aircraft have a cruise lift coefficient (C_L) less than 1.0. The exception is Global Hawk, which has a C_L twice as high as the other comparator aircraft. This is due to Global Hawk's small wingspan and relatively high weight. Table 1 lists the lift coefficients of the comparator aircraft.

Table 1: Lift coefficients of comparator HALE aircraft

Aircraft	**C_L**
Global Hawk (70 000 feet)	2.03
Helios (90 000 feet)	0.61
Centurion (90 000 feet)	0.96
Helios (100 000 feet)	0.79

In order to fly at a comparable C_L, the VT HALE aircraft was designed to fly with a C_L of 0.61.

3.2 Reynolds number

The Reynolds number is the ratio of inertia to viscous forces. It is an important parameter in determining similarity requirements, since the transition from laminar to turbulent flow boundary layer properties are functions of the Reynolds number. The Reynolds number is defined as:

$$\mathrm{Re} = \frac{\rho V l}{\mu}$$

where _ is the density, V is the velocity, l is the characteristic length (chord length of airfoil), and _ is the dynamic viscosity.

HALE aircraft fly at relatively low Reynolds numbers in the range of 200,000-350,000. Since our aircraft was to match the range of typical HALE aircraft, the comparator aircraft listed in Table 2 were used as a benchmark for our Reynolds number range. The VT aircraft was to be built to fly at a Reynolds number of approximately 250,000.

Table 2: Lift coefficients of comparator HALE aircraft

Aircraft	Re
Global Hawk (70 000 ft)	364 000
Helios (90 000 ft)	270 000
Centurion (90 000 ft)	205 000
Helios (100 000 ft)	214 000

3.3 Wing loading

Wing loading is the weight of the aircraft divided by the area of the wings. Wing loading therefore defines how much lift a given area of wing must produce. Since lift has equal weight in steady-state flight, it also bears strongly on the mechanical stresses and structural requirements of a wing. Wing loading is an important aerodynamic characteristic that must be paid attention to in scaling. It was therefore imperative that our wing loading matched the same range as HALE comparator aircraft. HALE aircraft

have relatively low wing loadings, under 1 lb/ft^2. Table 3 illustrates the wing loadings of comparator HALE aircraft.

Table 3: Wing Loading of comparator HALE aircraft

Aircraft	Wing Loading (W/S), ft/lb^2
Global Hawk	47.41
Helios	0.81
Centurion	0.66

Global Hawk has a very high wing loading due to its small wingspan and large weight, while HELIOS and Centurion fall in the average, below 1 lb/ft^2. The VT morphing HALE aircraft will fly at a wing loading of 0.81 lb/ft^2 to fit into the general wing loading range of current HALE aircraft.

4 Initial Aircraft Sizing – Matching Aerodynamic Similarity Criteria

In order to match the target Reynolds number, lift coefficient, and wing loading, four variables were looked at: span, weight, wing loading, and velocity. Since all variables are dependant of each other, a constraint plot was constructed to interpolate the relationships.

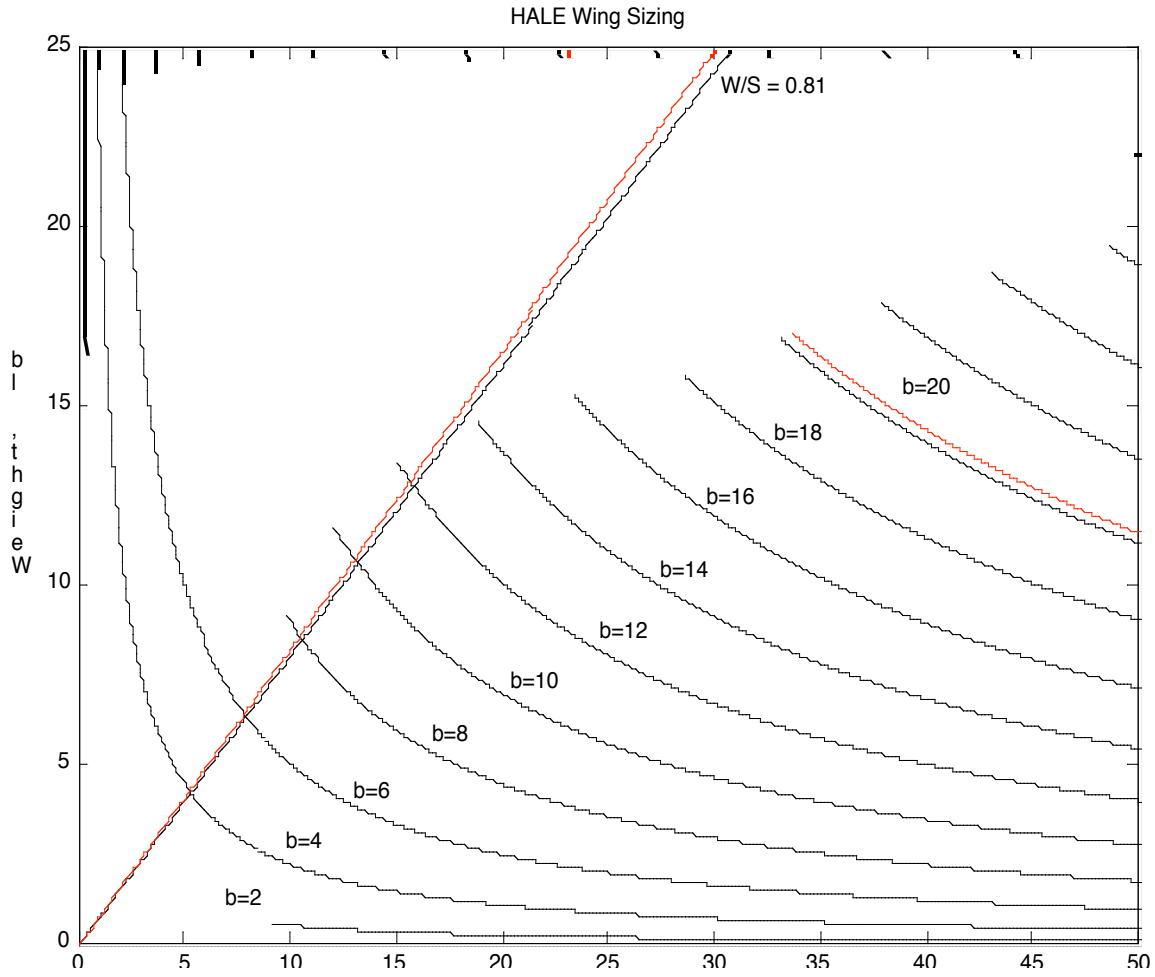

Figure 1: Constraint plot relating the span, weight, wing-loading, and velocity.

The wing loading, Reynolds number, and lift coefficient were fixed at 0.81 lb/ft^2, 250,000, and 0.61 respectively to match current HALE aircraft. The wingspan was limited to a maximum of 12 feet for construction space constraints. Holding these variables constant, the design weight, velocity, and wing chord were determined.

Aerodynamically matching current HALE aircraft drove the design weight to 15 lbs, design cruise speed to 20 mph, and wing chord to 1.3 ft. The resulting VT HALE aircraft design characteristics constrained by aerodynamic similarity are shown in Table 4.

Table 4: VT HALE characteristics

VT Morphing HALE Aircraft Characteristics	
Wing span	12 ft
Wing chord	1.3 ft
Weight	15 lbs
Wing loading	0.81 lb/ft^2
Lift Coefficient	0.61
Reynolds number	250,000
Cruise velocity	29 mph

5 Conceptual Design

Given the mission and RFP, the VT AE/ME Morphing Wing team brainstormed several conceptual designs for an R/C scale HALE aircraft. The team explored telescoping wing, folding winglet, and folding wing designs as methods of achieving a 300% increase in wingspan. The designs varied from single engine to multiple engine concepts encompassing several configuration options.

5.1 Folding Winglet

One concept investigated was the folding winglet (Figure 2). It featured a large telescoping winglet that would fold down and extend in flight, allowing a 250% increase in wingspan. This concept capitalized on the team's previous experience with telescoping wings on the 2002-2003 BetaMax. However, lack of structural integrity in the telescoping winglet sections was a disadvantage to this design. Additionally, the large size of the winglets would yield large friction drag. Although they would still provide the benefits of traditional winglets, such as reduced downwash or additional thrust, these effects would be mitigated due to the larger friction drag. The propulsion system consisted of three pod-mounted engines. The three engines added a significant amount of weight to the design and were determined unnecessary to the mission criteria since the aircraft would only be flying at low speeds.

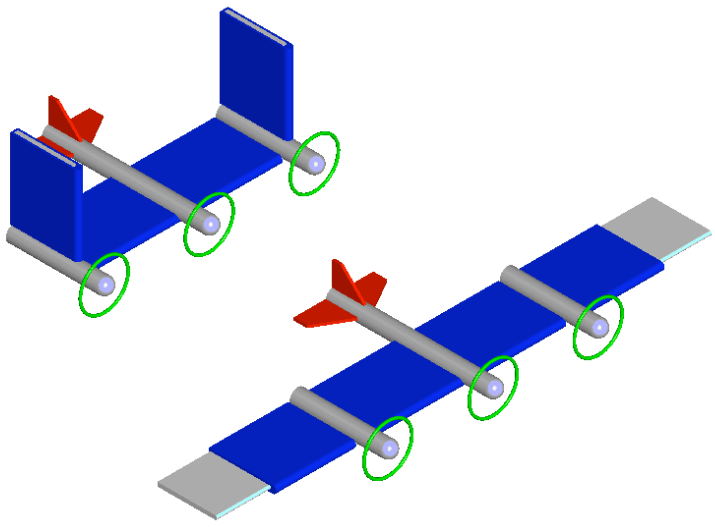

Figure 2: Folding Winglet Concept

5.2 Equilateral, Triangular Wing Concept

The equilateral, triangular wing concept was explored for its simple, folding wing design (Figure 3). Only two folding joints were needed to actuate the wing, and the structure could be attached at a top point to improve structural stability. The equilateral design would allow for the 300% wingspan increase desired. A single engine would propel the aircraft from a central fuselage extending to a conventional tail. There were two primary disadvantages to this design: its single engine was inadequate for the size of the aircraft and the large vertical side area was detrimental to lateral-directional stability.

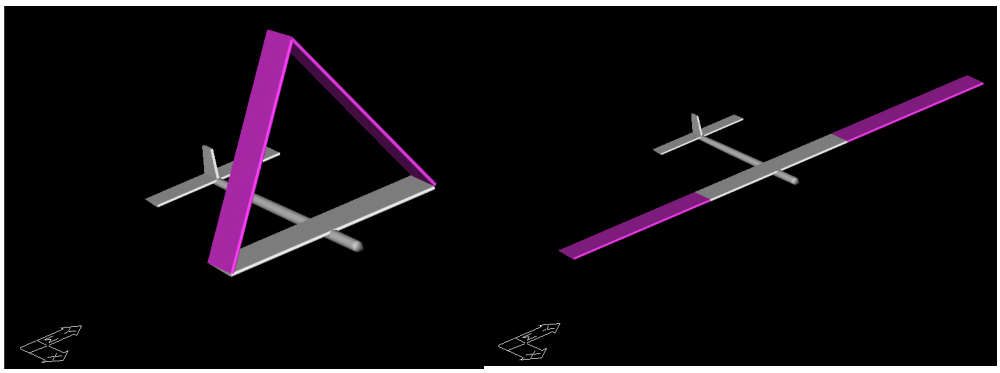

Figure 3: Equilateral, Triangular Wing Concept

5.3 Boom-e-rang Concept

The boom-e-rang concept was a single engine, telescoping, flying wing configuration (Figure 4). It allowed a 250% increase in wingspan and capitalized on the team's previous experience with telescoping wings and flying wing aircraft. However, this concept had many disadvantages. Motor mounting would be difficult since the entire wing would pivot about the nose. Flexible, advanced materials would be needed in the nose section. The aircraft would be inherently unstable because of its flying wing configuration and lack of a tail or vertical stabilizers. The actuators pivoting the wing

would have to act against the freestream velocity. Overall, this concept was not considered feasible.

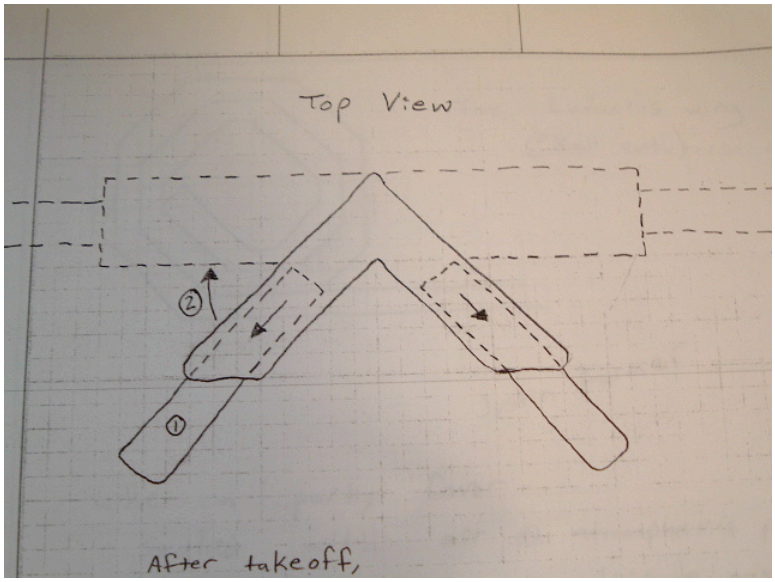

Figure 4: Boom-e-rang Concept

5.4 Biplane Concept

The biplane concept, shown in Figure 5, had the best performance characteristics for the retracted geometry. The concept featured an upper and lower wing. The upper wing would split in half spanwise and extend down, appending to the lower wing. Only a 200% increase in wingspan was possible with this design. The actuator arm would have to be extremely strong to support the wings during actuation, and it would create a tremendous amount of drag. Additionally, there would have to be an opening on the upper surface of the lower wing to conceal the actuator arm when extended; this would adversely affect aerodynamics.

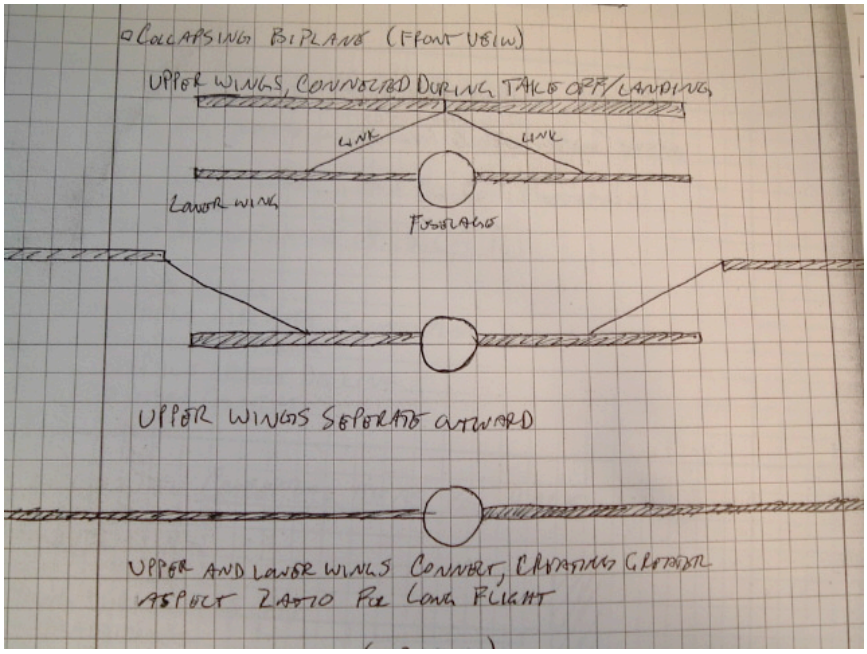

Figure 5: Biplane Concept

5.5 Folding Wing Concept

Another concept investigated was the folding wing concept (Figure 6). This concept had two joints where the wings folded, yielding less vertical side area than the equilateral design. A single motor located in the central fuselage would simultaneously actuate the wing. The propulsion system consisted of two engines, mounted on the innermost wing joints. When in the retracted position, the outboard wing sections would provide extra lift, much like a biplane. Additionally, outboard ailerons could be designed to assist the wing actuation mechanism by reducing the aerodynamic loading during extension and retraction. The three folding wing sections allowed for a 300% increase in span. The disadvantages of this concept were the additional joints required, wing skin interference at the joints, and a complex control system if aileron assistance were utilized.

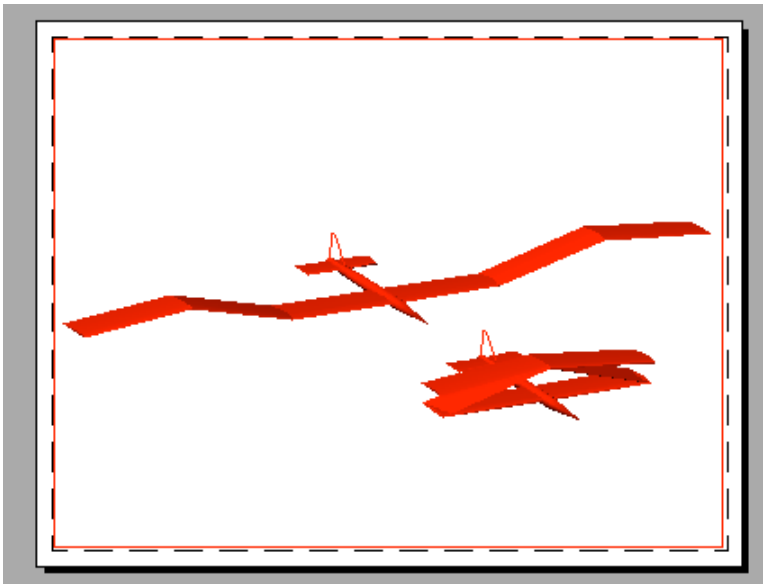

Figure 6: Folding Wing Concept

5.6 Concept Matrix

The five concepts investigated were ranked on a scale of 1 to 5 for span increase, weight, ease of construction, complexity, and stability and control. Span and weight were considered the most important factors in choosing a final design and were given a weight of 0.3 in the concept design matrix. The next most important factor was stability and control, which was given a weight of 0.2. Ease of construction and complexity, though important, were given a weight of 0.1 since the team had access to smart structures and advanced construction techniques. The advantages and disadvantages of each concept, as previously discussed, are summarized in Table 5. The folding wing concept was chosen as the optimum configuration.

Table 5: Conceptual Design Matrix

	Span	Wt.	Const.	Complex.	S & C	TOTAL
Weight	0.3	0.3	0.1	0.1	0.2	
Folding Winglet	3	2	3	2	3	2.4
Equilateral	5	4	4	4	2	3.9
Boom-e-rang	3	4	2	2	1	2.7
Biplane	1	2	2	4	5	2.5
Folding Wing	5	3	4	3	5	4.1

6 VT HALE Configuration

The final design was affectionately named “The Bangle” due to its odd shape which resembles a dance move from a 1980’s song, “Walk like an Egyptian” by the band *The Bangles*. The fuselage fitted to the aircraft spans 62.8 inches from the nose to a 13.7 inch high vertical tail. The wings have a chord length of 15.74 inches and a maximum thickness of 1.872 inches. A NACA 2412 airfoil was used for the inner and outboard wing sections, while a NACA 0012 airfoil was used for the mid-wing. Two Aveox motors with 12 inch diameter propellers are used to power the aircraft, mounted at the first joint 24 inches from the center of the fuselage on each side. A two dimensional, three view CAD drawing of the aircraft is shown in Figure 7.

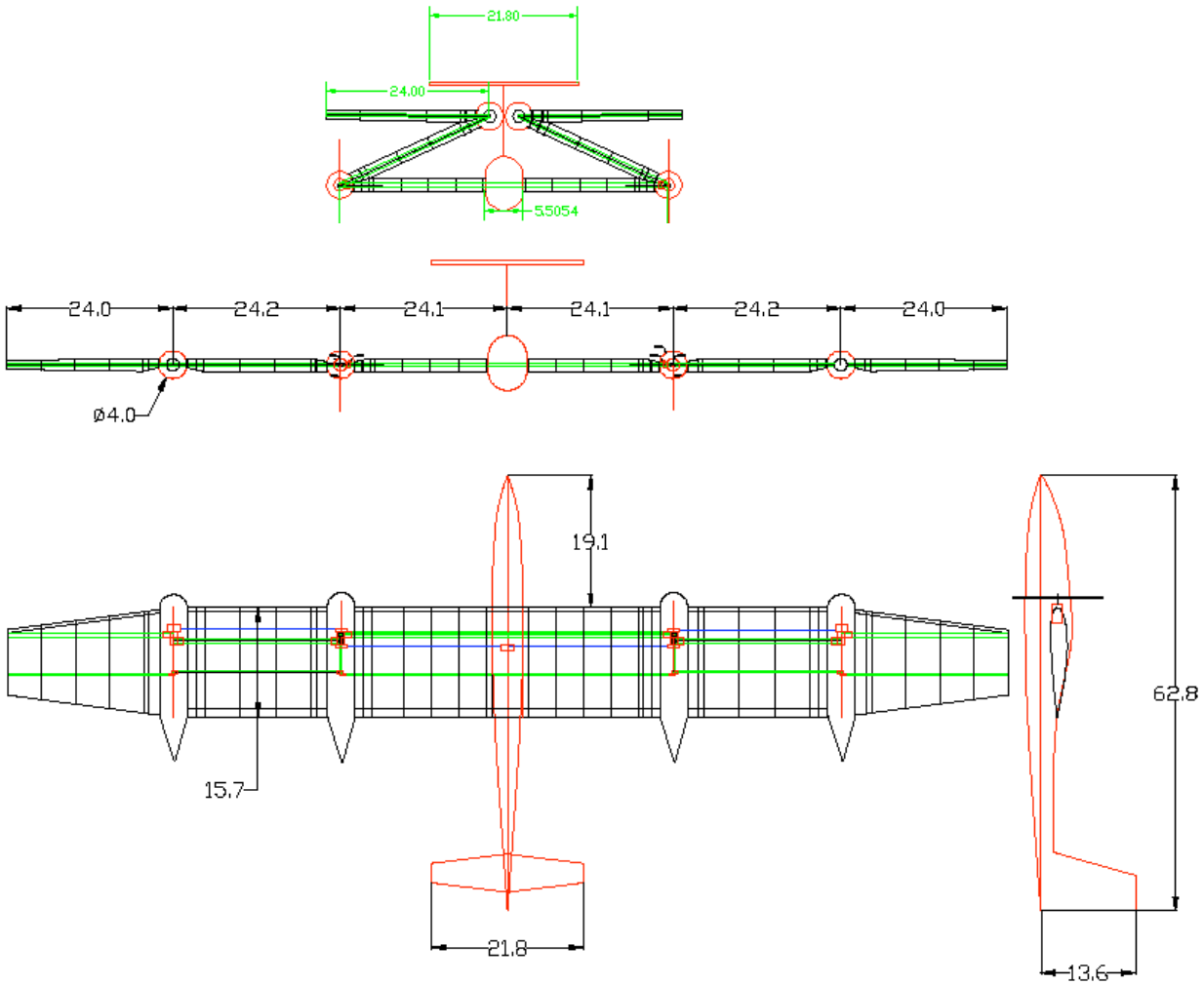

Figure 7: Three view CAD drawing using AutoCAD 2002 software.

The wings of the aircraft are divided into three sections. At takeoff, the wings of the aircraft are folded on top of each other to form an isosceles triangle with a 24 inch wing section extending horizontally from the top of the triangle on each side. The total wingspan at takeoff is 48 inches. After departure, the wings can be actuated through a system of pulleys to extend the wings for a maximum wingspan of 144.4 inches, providing the desired 300% span increase. The wings will lock in a horizontal position, and the aircraft will resume its ascension. A schematic drawing of the pulley-spar system can be seen in Figure 8.

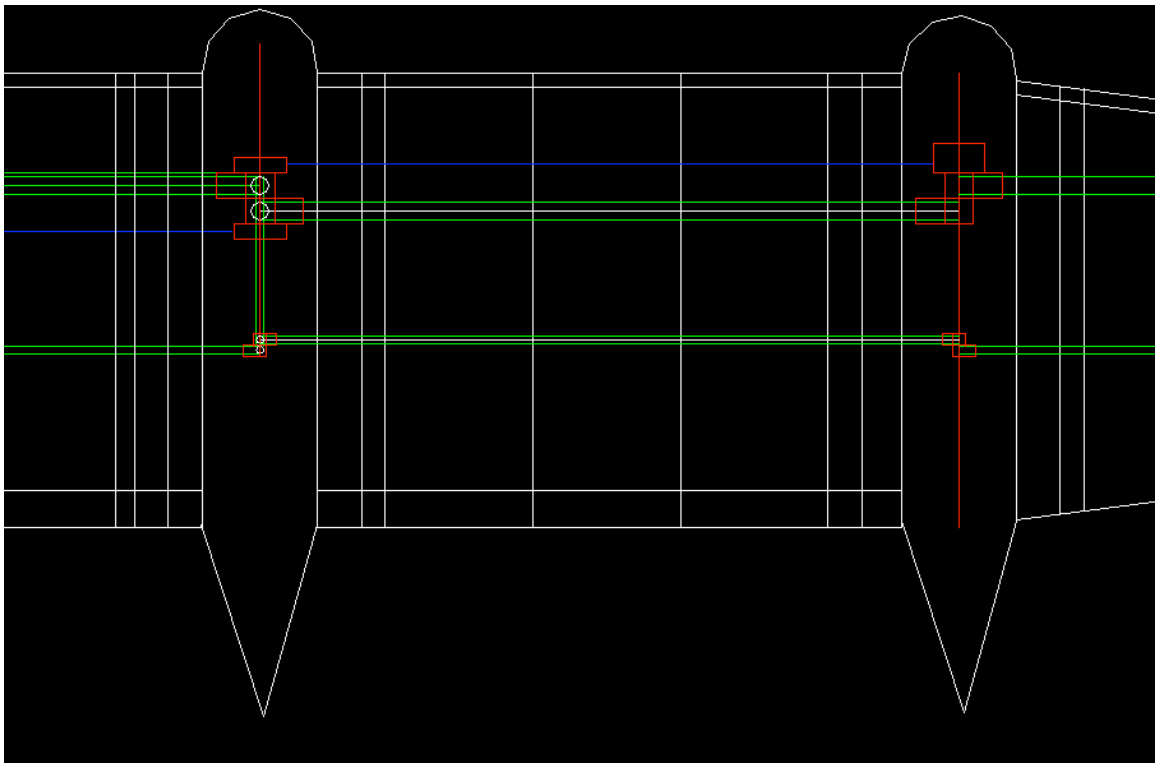

Figure 8: CAD drawing of pulleys located inside of the wing joints.

Four inch diameter pods were constructed to encompass the pulleys at each of the four joints. Figure 3 shows the dimension of this pod in relation to the pulley system. Six pulleys and ten spar joints machined out of Delryn® were used to join the main and rear spars within the pods. A steel wire cable with adequate load capacity was wound around the pulleys to drive the wings between their horizontal and retracted positions.

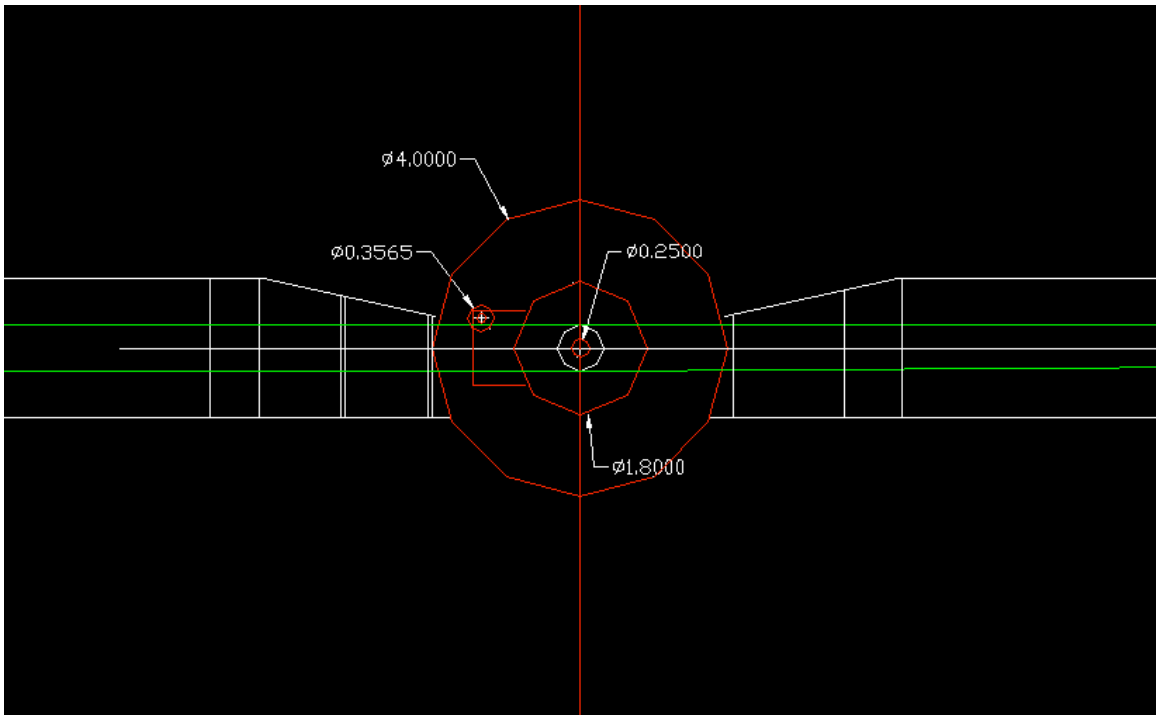

Figure 9: Front view of the first wing joint, showing pulley and pod diameters.

7 Structure

7.1 Wing Structure

7.1.1 Spars

A dual spar system was used to provide ample torsion and bending resistance in the VT HALE aircraft. Wrapped carbon fiber tubes were used for the spars due to their high strength in bending and light weight. The main spar, 0.625 inches in diameter, ran through the quarter-chord, while the 0.25 inch rear spar ran through the 6/10 chord.

The spars were designed to handle a maximum of 41.38 ft-lb and 16.25 lb shear that would be seen at a 2.5G wing loading. Figure 10 highlights the shear forces and bending moments along the span of the wing.

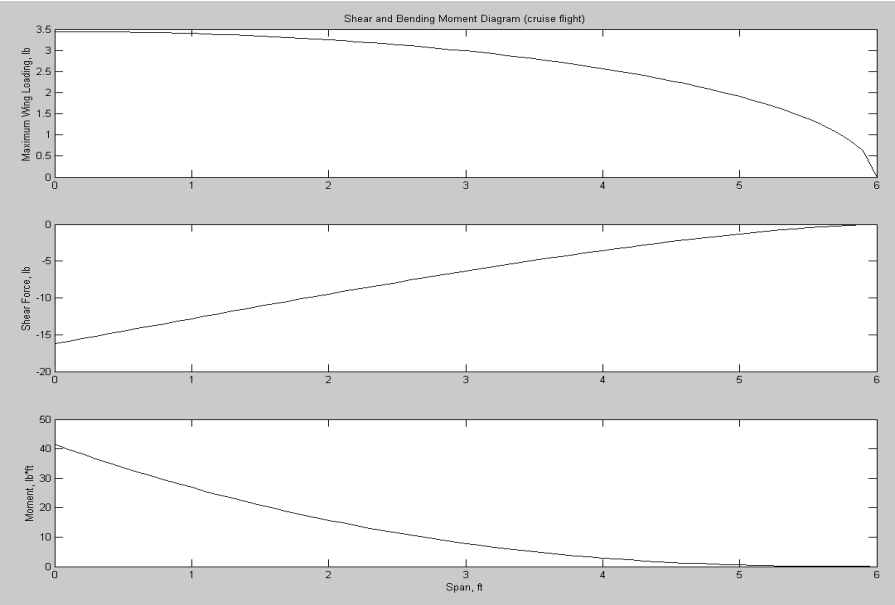

Figure 10 The loads on an extended wing

7.1.2 Ribs

Forty-six ribs were constructed out of 1/8 inch thick balsa to form the aircraft's 1.3 ft chord wing. The ribs were assembled in CAD drawings, then exported to a laser cutter that precisely formed the NACA 2412 and NACA 0012 airfoils. Each rib was manufactured with two holes that permitted the main and rear spars to slide through. A 2"x1" box was cut out of the ribs to allow the wires used in the wing extension system to slide through.

7.1.3 Torsion Box

A balsa box was constructed in the inner wings to aid in torsion resistance. Two 1/4"x 1/8"x 24" balsa beams were fitted at the 1/5 chord and 4/5 chord at the top and bottom of the wings. The beams were joined together by four crossing beams of the same size to form a torsion-resistance box. Three-quarter inch leading edge and 1 inch trailing edge balsa stock were used to aid in additional torsion support.

7.2 Fuselage

The Bangle utilized a pre-fabricated fuselage, modified to accommodate the six sectioned folding wing and flight systems. Figure 11 shows the unmodified DG-505 sailplane that was purchased from ICARE. Only the fuselage of the DG-505 shown was incorporated into the design. The wings were discarded. The high gloss, gel-coated, hollow fuselage provided a strong, yet lightweight structure capable of transporting all the necessary systems for flight.

Figure 11 Glider purchased, showing original wings

The fuselage housed a variety of mechanisms required for the Bangle to function properly. Figure 12 displays the location of the multiple mechanisms within the aircraft. A 5/8 inch and _ hole were drilled mid-height through the fuselage to permit the passing of the wing spars through the body. The motor used to drive the wing extension mechanism was mounted between the main and rear spar within the fuselage. Blocks of balsa were shaped to the contour of the fuselage side and epoxied in place to act as servo mounts. Servos to control the rudder and nose wheel were mounted to two balsa block mounts, located one and 15 inches forward of the aircraft's CG (CG located _" forward

of the _ chord) . The elevator actuation servo was mounted in the vertical tail. Two Lithium Polymer battery packs used to power the propulsion system were secured to the cockpit of the fuselage. The three 9V batteries to power the wing extension motor were mounted on top of the Lithium Polymer packs.

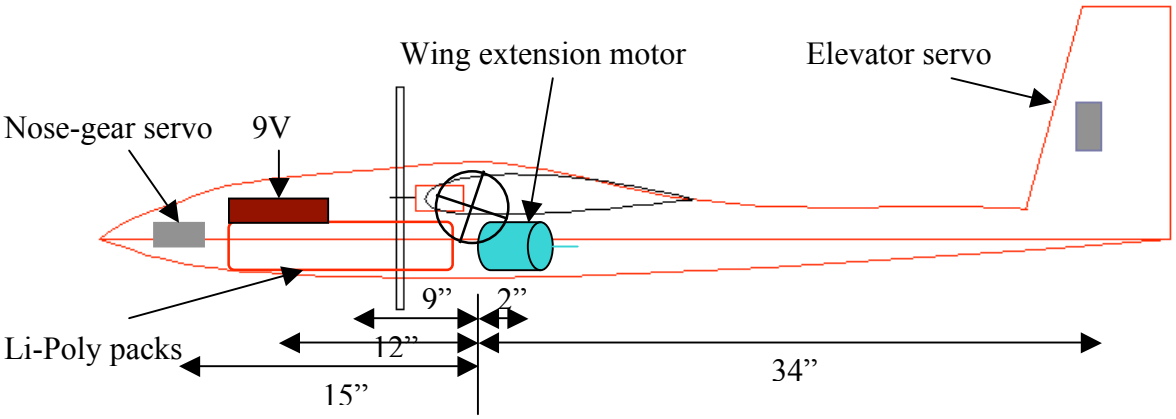

Figure 12: Side-view of fuselage showing component placements

8 Wing Extension System

8.1 Mechanics of system

A sketch of one side of the wing extension system is shown in Figure 13. For the sake of clarity, the middle wing section will be called Wing One, the next sections Wing Two and the outer sections Wing Three. Likewise the inner joints will be called Joint One and the outer joints Joint Two. The basic principle of operation was proposed by Dr. Charles Reinholtz and adopted by the team. This design involves using a cable and pulley system to extend the wings. The cable system is powered by a center driveshaft in the middle of the fuselage. A pulley on the driveshaft drives a cable that wraps around pulleys connected to Wing Two at Joint One. As the pulley attached to Wing Two

rotates, Wing Two is forced to rotate about Joint One. The outboard wings are not powered directly; instead a cable connects them to Wing One. In this section of the design, one pulley is fixed to Wing One, and another pulley is fixed to Wing Three. Since the cable around the pulleys is prevented from slipping, Wing Three cannot rotate relative to Wing One and always stays parallel with Wing One. This means that when the middle wing sections are rotated in the fully retracted position with the outer joint pods touching, the outer wing sections will be positioned much like the upper wing of a biplane. When the wings are fully extended, all wing sections are positioned to act as one straight wing.

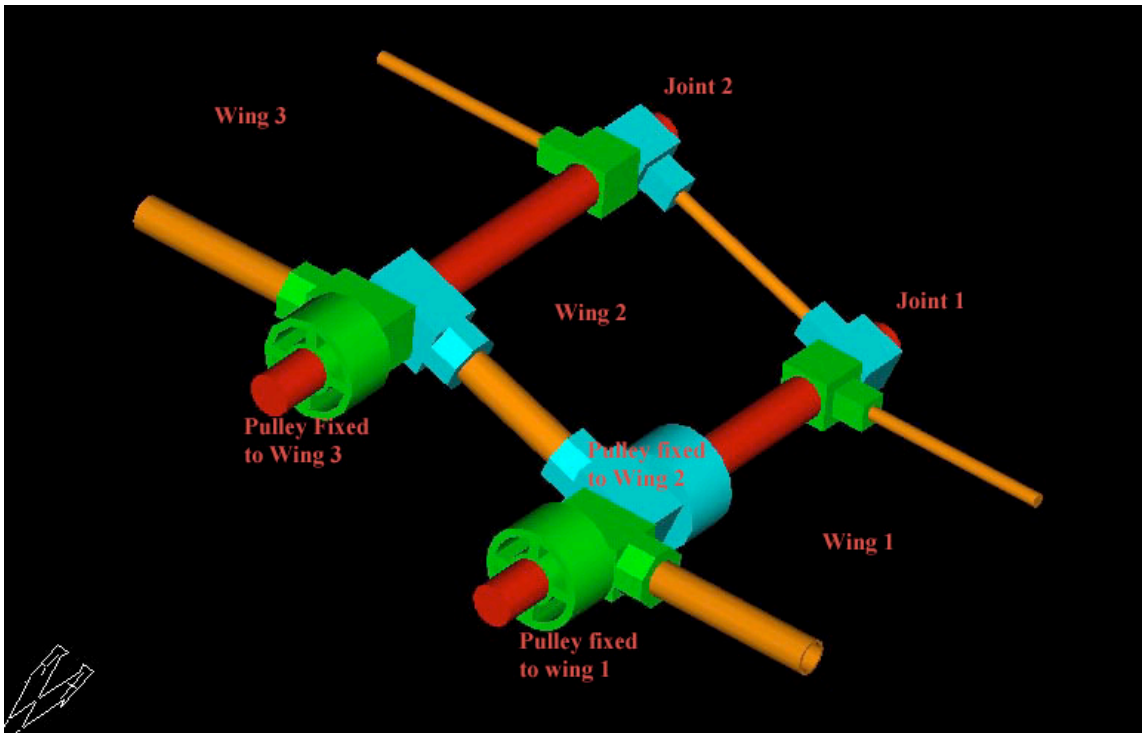

Figure 13: Sketch of one side of aircraft wing.

Analysis of our wing design determined that the pulleys must be able to handle the loads imposed on them aerodynamically at 2.5Gs, be lightweight, and be of a multi-wrap design. Since one pulley would be fixed to each individual wing section, it was

logical to use the main structural spars as points of attachment for the pulleys. The strongest feasible design was determined to consist of a cap to fit over the end of the spar, and a pulley machined from one block of material. The hinge pin at each joint would pass through the pulley/spar-cap and provide a pivot point at the center of the joints. This design can be seen in Figure 13. The pulleys were machined out of solid Delryn rod, first turning the pulley surface and cutting grooves for the multi-wrap cable design on a lathe, then machining the spar end-cap section of the part on a mill. Delryn was utilized as a material because of its relatively high strength and light weight compared to other alternatives. Delryn is also modestly priced and readily available. It was suggested that the team outsource the machining work to a local machine shop that could manufacture the parts on their CNC equipment. However the machine shop had an unacceptably slow turn-around time and a high cost. For these reasons the team machinist manufactured the parts in-house.

8.2 Motor to Drive System

A motor to drive the cable system was selected on the basis of torque, speed, weight, size, and current draw. The cable system used 1.8 inch diameter pulleys and was design to withstand a wing bending moment of 188 in-lb (2.5G loading) at the first joints. This meant that the cable system had to be capable of withstanding 188 in-lb of torque on the joint without failing. The system should also be expected to work at a 2 G loading. Since the pulleys were sized at 1.8 inch diameter, the cable tension would be equal to the required torque divided by the radius of the pulley, or 188 in-lb / 0.9 in = 209 lb of cable tension. The drive pulley, located in the fuselage, would have to power both wings. A

smaller diameter drive pulley was selected with a diameter of 1 in. The maximum force required by the pulley would then be equal to the sum of the torque required to move the wings, multiplied by the ratio of the radius of the drive pulley over the radius of the joint pulleys. This came out to be (188 in-lb x 2) x (.5 in / .9 in) = 208 in-lb of torque required from the cable drive system. Assuming again that the system must be able to withstand a 2.5G loading, but only be able to actuate under a 2G loading, the required drive cable torque would be 166.4 in-lb.

In selecting a motor for our application, Midwest Motion was found to carry the most suitable gearmotors and was capable of delivering within the necessary time frame. A gearmotor was purchased from Midwest that was only rated at 15 in-lb of output torque, but was capable of producing 78 in-lb of torque for very short durations. The gearmotor was received at a weight of 18.6 oz. By removing excess material, the team machinist was able to reduce the weight of the gearmotor by 3 oz to bring the total weight to under a pound. The motor was then light enough to suit the team's purposes, but was not capable of producing the required amount of torque. For this reason it was necessary to add a spur gear reduction with a 7:1 ratio after the motor. Assuming the spur gear reduction has an efficiency of approximately 70%, the gearmotor shaft would be required to deliver 33.5 in-lb of torque at a 2G loading and 42.4 in-lb of torque at a 2.5G loading. This value is well within the design limits of the gearmotor.

The motor was purchased with an output speed of 64 rpm. After going through the 7:1 reduction the cable drive shaft speed was reduced to 9.1 rpm. Due to the difference in drive pulley and joint pulley size, the wing joints have a rotational velocity of 5.1 rpm, and will travel the required 154º of rotation in approximately 5 seconds. A

picture of the gearmotor, gearmotor mount, gear reduction, and drive shaft with pulley is shown in Figure 14.

Figure 14: Motor and gearing installed into fuselage. Pulley to drive wings hidden behind white spur gear.

8.3 Drive System Power and Endurance

Three 9V batteries in series are used to provide electrical power for the gearmotor. At the working loads for the system, the gearmotor is rated to consume approximately 3.5 amps with an input of 27 volts. Since 1200 mAh, 9 V batteries are available with a weight of 1.3 oz, the gearmotor can be powered for over 20 minutes with a 3.9 oz battery pack.

8.4 Loads imposed on system

8.4.1 Aerodynamic Loading

The wing loading was a critical design characteristic for the aircraft. It determined the cruise speed, stall speed, and the extent to which turbulence affects the airplane. The wing loading is defined as the weight of the aircraft divided by the area of the wing.

The plane must be operated within the design limit load factor. An aircraft's strength is measured by the total load the wings are capable of carrying without distortion, permanent damage, or structural failure. The criterion for this plane was set using a limit load factor of 2.5. Thus, the wings must be able to extend and retract when forces 2.5 times greater than the weight of the aircraft were applied.

An analysis was performed in MATLAB, as shown in Figure 15, to calculate the maximum wing loading, the shear force, and the bending moment per foot of wingspan for each wing. The span shown in the figure begins at the wing root and extends to the wing tip. The airfoil sections were split into three parts along the semi-span for folding. Section joints occurred every two feet.

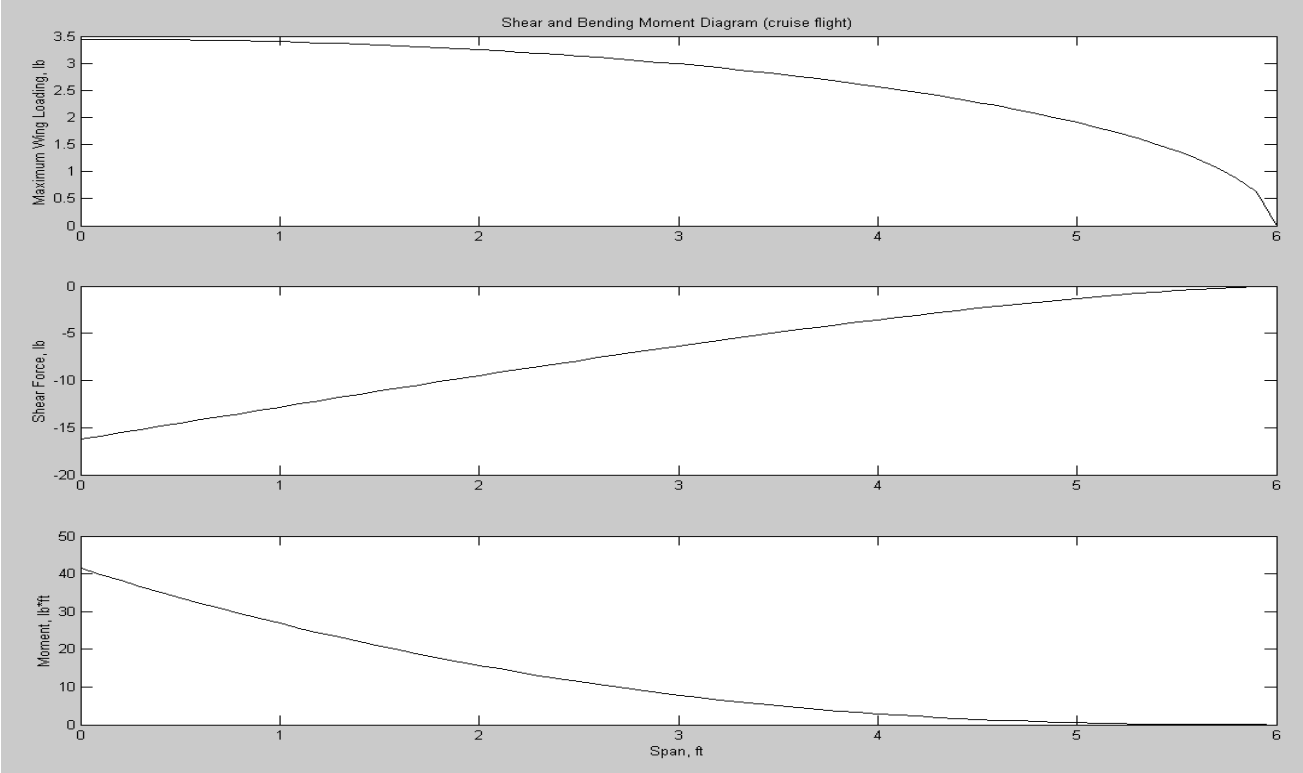

Figure 15: Maximum Wing Loading, Shear Force, and Moment versus Span.
The maximum bending moment at the root, the first hub, and the second hub are 41.38, 15.71, and 2.89 pound-feet, respectively. The maximum shear force at these locations is -16.25, -9.48, and -3.56 pounds, respectively.

The maximum shear and bending moments due to the aerodynamic loads occurred at the root. The maximum moment was 41.38 lb-ft, while the shear at the root was –16.25 lbs. Joint 1 had to sustain a 15.71 lb-ft moment and –9.48 lb shear. Joint 2 felt a smaller load, having to uphold a moment of 2.89 lb-ft and shear force of –3.56 lb.

8.4.2 Buckling Concerns

A major concern for the wings was the buckling of the spars. The spars needed to be lightweight yet strong. Carbon fiber tubes were used to provide extraordinary strength to weight ratios. The carbon fiber tubes were manufactured by pulling carbon fiber and venylester through a die of the desired cross section that formed a densely reinforced carbon composite that provided excellent tensile, compressive, and transverse strength.

The tubes chosen had an outside diameter of 0.625 inches and a thickness of 0.125 inches. Young's modulus for the material is 17.8 msi while the shear strength is 9.50 ksi. The fibers were wrapped, perpendicular to the length of the tube. Critical pressure of the material over the two foot sectioned spar lengths was of concern for the buckling analysis. This critical pressure was calculated using Equation 1.

$$P_{cr} = \frac{\pi^2 EI}{l^2}$$

Equation 1

where P_{cr} is the critical pressure, E is the young's modulus, I is the moment of inertia, and l is the length of the section. The moment of inertia is calculated by

$$I = \frac{\pi(OD^4 - ID^4)}{4}$$

Equation 2

where OD is the outside diameter of the tube, and ID is the inside diameter of the tube. Upon completion of these calculations for a 2 ft spar, I equaled 4.422 E-3 in^4, and the critical pressure was found to be 337 lbs.

9 Aerodynamics

9.1 Airfoil Selection

Due to the limited time allotted for detailed design of the Bangle, a thorough airfoil selection process was not feasible. Additionally, since the Bangle's endurance was limited primarily by the propulsion system, selection of a highly efficient airfoil was unnecessary. The team needed an airfoil that was proven reliable for low speed aircraft. The NACA 2412 was chosen as a sufficient airfoil for the Bangle. The NACA 2412 has been used on several general aviation aircraft, particularly on several Cessna single-engine aircraft and the ultralight Ikarus C-42 (Lednicer). However, based on the recent advances in design and optimization of natural laminar flow airfoils, the team recommends use of at least a NACA 6-series airfoil for a full-scale configuration. The lower drag provided by a carefully chosen natural laminar flow airfoil would allow longer endurance when used with an adequate propulsion system on a full-scale HALE aircraft.

The performance characteristics of the NACA 2412 airfoil are shown in Figure 16; the lift curve, pitching moments, and drag polar are shown for a Reynolds number of 250,000, which is approximate for both takeoff and cruise conditions. The NACA 2412 has a C_{Lmax} of 1.3 and minimum drag of 85 counts as shown in Figure 16.

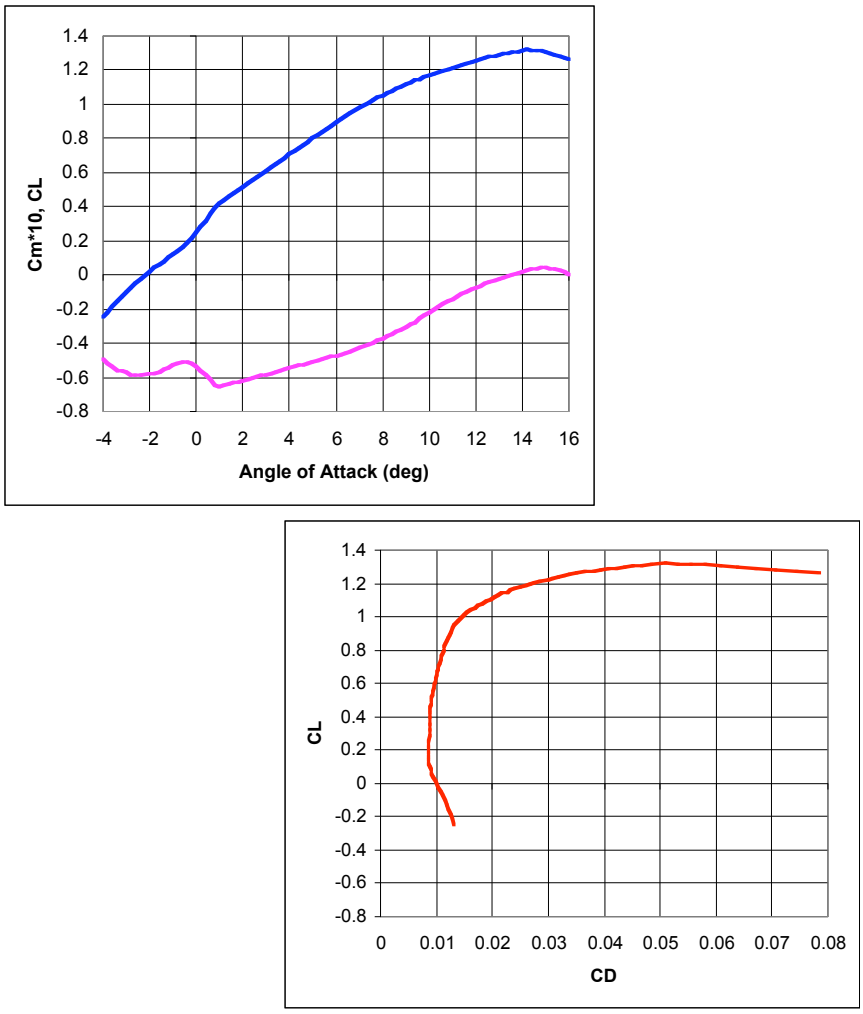

Figure 16: Airfoil Characteristics (Reynolds Number = 250,000)

In the center sections of the wing, a cambered airfoil was undesirable since this section would experience extreme dihedral changes. A NACA 0012 symmetric airfoil was chosen for this section to match the airfoil thickness in the inboard and outboard sections. The effect of varying the airfoil on the span loading was calculated in Tornado and is shown in Figure 17. The decreased lift caused by the center sections would lower the span efficiency during cruise, but was a necessity for adequate morphing performance.

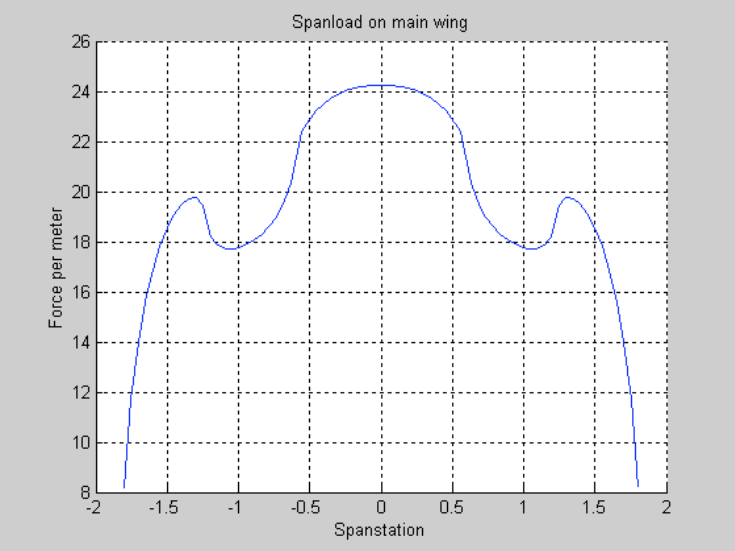

Figure 17: NACA 2412 and NACA 0012 airfoil effect **on span loading**

9.2 Drag Buildup

The zero-lift drag was estimated using the component buildup method (Raymer). Zero-lift drag of the fuselage, wing, tail, wing pods, and landing gear was estimated using the flat-plate skin-friction drag coefficient and a form factor, as described by Equation 3.

$$C_{D0} = \frac{1}{S_{ref}} \left\{ \sum \left(C_{f_c} FF_c S_{wet_c} \right)_{w,f,HT,VT,p} + 2 * 0.25 S_{frontal_{mainLG}} + 0.25 S_{frontal_{nnoseLG}} \right\}$$

Equation 3

Interference effects were neglected in the zero-lift drag calculation, and wetted areas of the wing and tail sections was estimated as twice the planform areas. The breakdown of each component's drag contribution is shown in Table 6. The total zero-lift drag coefficient was 0.0210 for the Bangle.

Table 6: Zero-lift drag buildup

Component	C_{D0}	Percentage of Total Drag
Wing	0.0124	59.0
Fuselage	0.00363	17.3
Horizontal Tail	0.00063	3.0
Vertical Tail	0.00043	2.0
Wing Pods (4)	0.00086	16.4
Main Gear (2)	0.00017	1.6
Nose Gear	0.00008	0.4
TOTAL	*0.0210*	*100*

After determining the zero-lift drag contributions, induced drag was added to complete the drag buildup analysis. The induced drag is defined in Equation 4.

$$C_{Di} = \frac{C_L^2}{\pi A \mathrm{Re}}$$

Equation 4

The efficiency factors, e, were calculated for both the cruise and takeoff configurations. The cruise configuration efficiency was calculated for a straight-wing aircraft, and the takeoff configuration efficiency was calculated with the biplane span efficiency factor equation (Raymer). These equations are given below (Equation 5-Equation 6), where _ is the ratio of the shorter span to the longer span of the biplane, r is the ratio of the lift on the shorter wing to longer wing, and _ is an interference factor. _ was determined from Figure 12.34 in Raymer.

Straight Wing: $e = 1.78\left(1 - 0.045 AR^{0.68}\right) - 0.64$

Equation 5

Biplane: $e = \dfrac{\mu^2 (1+r)^2}{\mu^2 + 2\sigma\mu r + r^2}$

Equation 6

The span efficiencies were determined to be 0.78 and 1.43 for the cruise and takeoff configurations, respectively. Figure 18 shows the final total drag polars for the cruise and takeoff configurations. The aspect ratio of the takeoff configuration was determined by the square of the span divided by the total area of horizontal wing sections. There is a significant drag reduction for the cruise configuration, which illustrates the benefit of morphing. The drag at takeoff is particularly high because of the induced drag, amounting to 8.4 lbs. The power of the two Aveox engines is enough to counteract the drag, allowing for takeoff. The takeoff performance is further discussed in the Performance section.

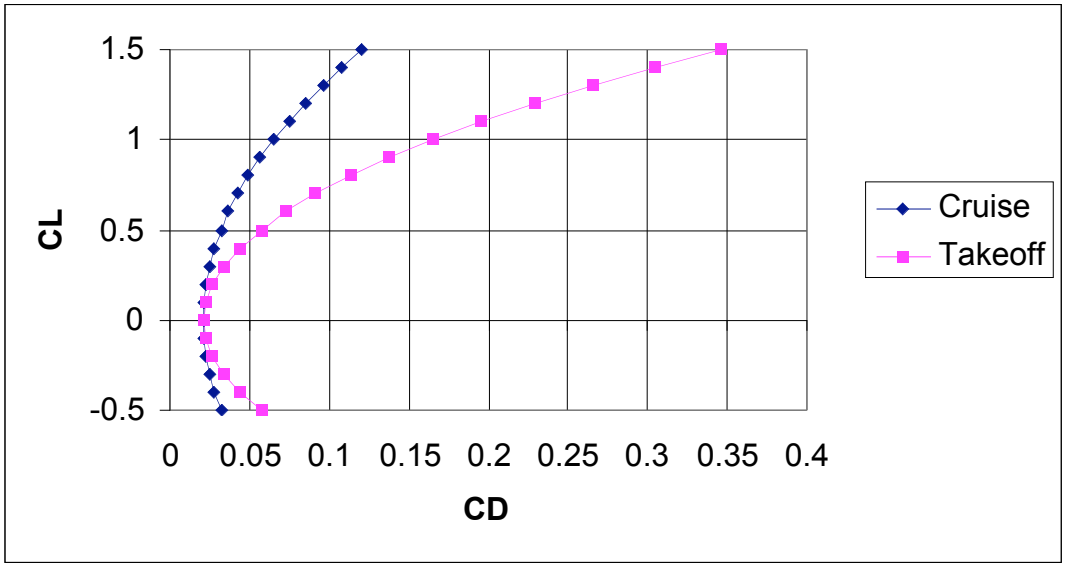

Figure 18: Drag Polar Comparison for Takeoff and Cruise Configurations

10 Stability and Control

The stability characteristics of the Bangle were calculated using two different vortex lattice codes (VLM). Tornado, the first code used, is a MATLAB code that calculates stability derivates using the slope of the camber line for NACA 4-digit series airfoils (Melin). The second code used was JKayVLM, which is based on flat plate assumptions (Kay). Two codes were used because JKayVLM could not calculate the stability derivatives for the retracted Bangle geometry, and comparison of the two results for the extended and 90º geometries provided better confidence in the predictions.

The stability derivatives indicated in Table 7-Table 9 are given for the extended configuration for cruise condition, retracted configuration for takeoff and landing, and for the 90º retracted configuration, which was the worst case for lateral-directional stability. These stability derivatives indicated that the Bangle was stable in all important flight conditions for the three geometries studied.

Table 7: Stability Derivatives for Extended Geometry (Cruise)

Longitudinal Derivatives		**Lateral-Directional Derivatives**	
$C_{L\_}$	7.34	$C_{n\_}$	0.026
$C_{m\_}$	-1.02	$C_{l\_}$	-0.0071
C_{m_e}	6.99	C_{n_a}	-216
Static Margin (%)	13.8	C_{l_a}	0.42
		C_{n_r}	-0.197
		C_{l_r}	0.0504
		C_{lp}	-0.82

Table 8: Stability Derivatives for Retracted Geometry (Takeoff and Landing)

Longitudinal Derivatives		**Lateral-Directional Derivatives**	
$C_{L\_}$	5.80	$C_{n\_}$	0.13
$C_{m\_}$	-1.68	$C_{l\_}$	-0.42
C_{m_e}	-1.754	C_{n_a}	-0.028
Static Margin (%)	29.0	C_{l_a}	0.256
		C_{n_r}	-0.157
		C_{l_r}	0.044
		C_{lp}	-1.07

Table 9: Stability Derivatives for 90° Retracted Geometry (Worst Case Scenario)

Longitudinal Derivatives		**Lateral-Directional Derivatives**	
$C_{L\_}$	8.33	$C_{n\_}$	0.023
$C_{m\_}$	-2.45	$C_{l\_}$	-0.0071
C_{m_e}	-1.758	C_{n_a}	-0.025
Static Margin (%)	29.4	C_{l_a}	0.388
		C_{n_r}	-0.174
		C_{l_r}	0.0504
		C_{lp}	-0.18

The fuselage and tail portions of the aircraft were prefabricated, which left little room for optimum sizing of control surfaces. Therefore, stability analysis was performed for the morphing wing implemented on the prefabricated fuselage. Concern was raised regarding the small empennage section, particularly for the elevator effectiveness; the aircraft needed enough nose-up pitch on takeoff to counteract the large static margin of the retracted geometry. With an elevator effectiveness of approximately -1.75, the

prefabricated control surfaces were determined adequate for takeoff. Tornado analysis of maximum up and down elevator deflection supports this conclusion (Figure 19). Only a small elevator deflection is necessary to allow trimmed flight for takeoff rotation.

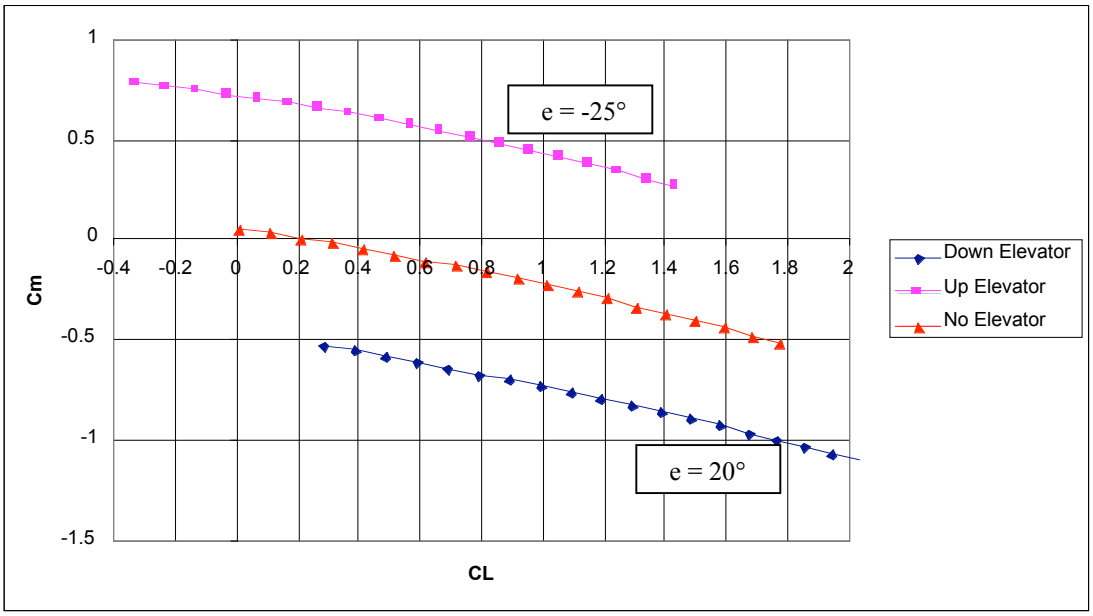

Figure 19: Elevator Trim Analysis

The team debated whether or not to include outboard ailerons in the design. The additional set of ailerons would provide more control authority for the extended cruise configuration and would alleviate loads on the wing extension mechanism during geometry transition. Outboard ailerons would also increase the weight of the wing and require the use of a more sophisticated flight control system. The use of inboard ailerons only would reduce overall weight of the wing, but require the ailerons to encompass a large percentage of the chord in order to provide enough roll control with the wings extended. With an aileron chord that was 35% of the wing chord, the Bangle had a predicted steady state roll rate of 127 deg/sec for a maximum aileron deflection of 30º.

This was determined adequate for the mission, and thus only inboard ailerons were incorporated on the design.

11 Performance

11.1 Constants

During all test flights the aircraft will be flown at an altitude of approximately 2000 ft. The estimated final weight, W, of the aircraft was 17 lbs. From the aerodynamic analysis and the use of a NACA 2412 airfoil the maximum lift coefficient (Cl_{max}) was determined to be 1.3, a drag coefficient (C_d) of 0.25 and the aerodynamic efficiency of 1.43 at take off. From the sizing requirements a cruise lift coefficient ($C_{Lcruise}$) of 0.61 was used. The area of the wing in the retracted configuration was 10.35 ft^2. Assuming the worst case scenario of taking of in long turf, a ground coefficient of 0.08 was used for the take off and landing calculations.

11.2 Stall and Cruise Velocities

The stall speed is the speed at which the aircraft stalls at C_{Lmax}. It was calculated using the equation:

$$V_{stall} = \sqrt{((2W)/(\_ S C_{Lmax}))}$$

Using the constants noted above, the stall speed, V_{stall}, was determined to be 33.6 ft/s.

The cruise speed was calculated using $C_{Lcruise}$ of 0.61. Inputting this value along with the required constant into the equation:

$$V_{cruise} = \sqrt{((2W)/(\_ S C_{Lcruise}))}$$

led to a cruise velocity of 49.0 ft/s.

11.3 Take-off Roll

It was a necessity that the Bangle take off in a short distance in its high wing loading situation with wings retracted. All flight tests were conducted at the Christiansburg airfield in Christiansburg, VA, with a grass runway 400 ft in length. The following calculations assumed that the take off was conducted during calm winds.

The first step in calculating the take-off roll distance was to calculate the take-off speed, V_{TO}. Since the stall speed is the lowest speed at which an aircraft can take off, the take off speed was set at $1.15*V_{stall}$. This factor allowed for unexpected gusts so that the aircraft would not stall on take-off. Using this factor the take-off speed was 40 ft/s.

Analysis of the power system through P-calc supplied by Diversity Model Aircraft noted that each motor would produce a static thrust of 6.5 lbs and a static power of 502.3 W. The motors have an efficiency of 88.7%. These numbers were calculated using a 13"x8" propeller. The power available, P_{avail}, at the take-off speed is:

$$P_{avail} = \_pP_s$$

where $\_p$ and P_s are the efficiency of the motors and the static power, respectively. From this the thrust at take-off, T_{TO}, can be calculated using the relationship:

$$T_{TO} = P_{avail}/V_{TO}$$

giving a take-off thrust of 17.0 lbs.

The lift coefficient for a minimum ground run is determined by:

$$C_{Lg} = \_/2K$$

Where _ is the ground coefficient and K is $1/(\pi ARe)$.

Using these values along with the constant previously mentioned, the ground roll distance, S_{roll}, can be calculated using:

$$S_{roll} = (1/B)*\log(A/(A-(B*(V_{TO}^2))))$$

where

$$A = g.*((Ts./W)-\_)$$

and

$$B = (g/W).*((^1/_2*\_*S.*(C_{dTO} - (\_*C_{Lg})))+a);$$

where g is the gravitational constant, and a is a constant associated with the thrust. Using this equation rendered a ground roll distance of 116.3 ft.

The take off roll was also calculated for a 12"x8" propeller. In this configuration, each motor produced a static thrust, T_s, of 5.6 lbs, a static power, P_s, of 394.5 W and an efficiency of 87.3%. Using the same procedure above to determine the take-off distance, the 12"x8" propeller was analyzed and yielded a take-off thrust of 13.1 lbs and a take-off ground roll of 123.6 ft.

The 12"x8" propeller was chosen as the ideal propeller for the test flight providing the gross weight of the aircraft did not exceed 17 lbs. The propeller allowed for longer flight endurance but required a longer ground roll. Though the ground roll was longer, it was not significant enough to warrant increasing the size of the propeller unless the gross weight of the aircraft exceeded 17 lbs.

The landing ground roll of the aircraft was calculated without the use of brakes in the wings retracted position. Only friction and drag will slow the aircraft on arrival. Once again the constants noted above are being used and it is assumed that there will be no wind during the landing.

The same equation for the take-off roll was used for the landing roll, but thrust was set equal to zero at landing. Applying this equation yielded a landing roll of 138.8 ft.

12 Propulsion

The aircraft's propulsion system had to supply a large amount of thrust monopolizing a minimal part of the aircraft's weight. The system was required to provide a static thrust to weight ratio of at least 0.65 for short takeoff rolls, provide adequate thrust for a 29 mph cruise (44 ft/sec), and yield an endurance of 10-20 minutes. To better model current electric-powered HALE aircraft, gas engines were disregarded. Only electric motors were considered for propulsion. A summary of the propulsion system components is listed in Table 10.

Table 10: Propulsion system components

COMPONENT	MANUFACTURE & TYPE	SPECIFICAITONS
Motors	(2) Aveox F12S	Gearing: 3.7:1 internal Thrust: 89.2 oz (12x8 prop) Weight: 8.6 oz Max current: 56 amp (cont) Size: 1.1" (dia) x 2.6"
Batteries	(2) Thunder Power 4S4P Lithium Polymer battery packs	Max current: 60-70amp (cont) Voltage: 15V (3.7V/cell) Weight: 22.0 oz Size: 10.25"x2"x1"
Electronic Speed Controller	(2) Aveox SH-48	Max current: 40 amp (cont) Cell capacity: 10-30 Weight: 1.7 oz Size: 3"x3/8"x1/2"
Propellers	(2) APC 12"x8" and 13"x8"	Endurance with 12"x8": 45 min, 36 sec Endurance with 13"x8": 28 min, 48 sec

12.1 Motors

No single engine could provide the combination of thrust and endurance, and keep the system weight to a minimum. As a result, a multi-engine configuration was established. Two Aveox F12S geared electric motors were purchased through Diversity Model Aircraft in San Diego, California to power the aircraft. The F12S is a 36/24/1.5 motor with built-in 3.7:1 gearing. Internal gearing minimized the motors weight and provided a means for turning a larger propeller to gain more power. The Aveox F12S was the lightest commercially available motor that could meet the thrust and endurance design constraints. The motors weighed only 8.6 oz each. They each provided a static-thrust of 103.4 oz and in-flight thrust of 65.0 oz, equating to a 502.3 W power output per engine.

The motors had the capacity to run at an 89.5% maximum efficiency. At takeoff the engines ran close to their max efficiency at 88.7%. The motors were less efficient at cruise, maintaining an efficiency of 70.9%. The motors were unable to achieve a higher efficiency at cruise due to the size of the propellers. To increase motor efficiency at cruise, the propeller diameter and pitch had to be increased. Doing so would have lowered the endurance to a less than acceptable time.

12.2 Batteries

The F12S motors could handle a large voltage range but required at least 13 V to operate at full-power. NiCd, NiMH, and Lithium Polymer cells were considered for the power supply. 1.3 V NiCd and NiMH cells were cheap and had a high discharge rate that allowed for high current flow, up to 100 amps continuous. The lightest cells in this grouping weighed 2.2 oz. Eleven cells in series were necessary to provide 13 V to the

motor. Four sets of the eleven-cell packs in parallel per engine were necessary to yield fifteen minute full-throttle endurance. The resulting power supply if NiCd or NiMH cells were used would have been a total of 88 cells weighing a combined 12 lbs, manipulating 92.3% of the entire aircraft's weight. Consideration of these cells was immediately dropped due to their weight.

3.7 V Lithium Polymer cells provided far more power per pound than their nickel-based competitors. Each cell had a 2000 mAh capacity and weighed only 1.3 oz per cell (0.35 oz per volt). Though the cells could only handle 60-70 amps continuous (80 amp peak) draw from the motors, their high energy density made them the optimal power supply for the propulsion system.

Thirty-two Thunder Power 3.7 V Lithium Polymer cells were used to power the F12S engines. The cells were arranged into two battery packs containing 16 cells each. In each pack, four cells in series were stacked four layers in parallel (4S4P) to provide 15 V and sufficient endurance to the motors. The packs were purchased pre-soldered and packaged from Model Machining Services in Costa Mesa, California. Each weighed 22 oz and measured 10.25"x2"x1". One 4S4P pack was used per engine.

12.3 Electronic Speed Controllers and System Wiring

Use of Lithium Polymer cells limited the maximum continuous current draw to 70 amps. Optimally, the motors would have been wired in parallel, drawn their power from a single power source, and have been controlled by one speed controller. Placing the two considerably large F12S engines in parallel however required a high current. At full power, the engines would have drawn over 200 amps. The Lithium polymer cells, nor

any speed controller, could operate with such high current. As a result, the motors and power supplies were split into completely electrically independent systems.

Two Aveox SH-48 brushless electronic speed controllers purchased through Diversity Model Aircrafts were used to control the motors. The speed controllers could handle a continuous current of 40 amps (60 amp peak) and 10-30 Lithium Polymer cells. They weighed 1.7 oz each and measured 3”x1 3/8”x1/2”. The wiring schematic of the propulsion system is shown below in

Figure 20. The speed controllers each controlled only one engine and received power from one 4S4P battery pack to keep the systems electrically independent. The speed controllers were linked together to receive the same information from the aircraft’s receiver through a Futaba Y-harness. Linking the units in this fashion assured both speed controllers received identical commands thus leading to symmetric power output from the engines.

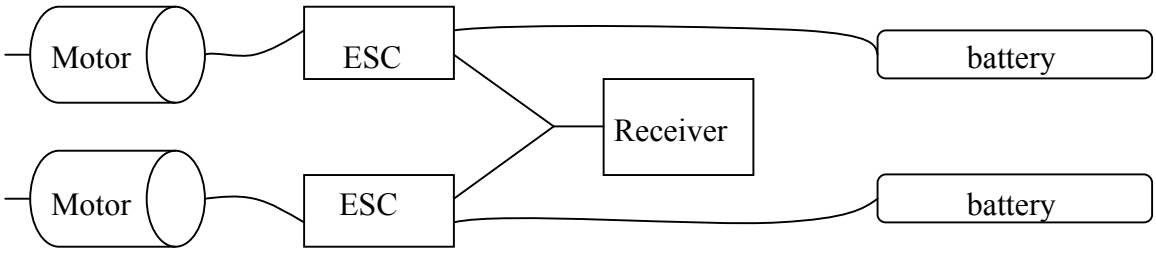

Figure 20: Propulsion system wiring diagram

12.4 Propellers

The propellers were sized based on the motor, power required, and endurance restrictions. The aircraft’s power requirements were limited by takeoff. A static thrust to weight ratio of at least 0.65 was necessary to assure short takeoff rolls. Propellers under 12” diameter could not provide enough thrust to meet the restriction. Using a 3.7:1

geared motor permitted the use of large propellers. The F12S could turn a 15" diameter propeller to produce a substantial amount of thrust, but the endurance would have been considerably short. As propeller size increased, power increased, but endurance decreased.

Two propellers offered near-desired performance, the 12"x8" and 13"x8". The 12"x8" provided a static thrust of 89.2 oz per engine, equating to a static thrust to weight ratio of 0.62 at the aircraft's maximum weight. This propeller would have given the aircraft a 14 min, 4 sec endurance. The 13"x8" propeller outputted 103.4 oz thrust per engine, and yielded a static thrust to weight ratio of 0.72 (at 18 lbs) and full-throttle endurance of 10 mins, 36 sec. The 12"x8" propeller gave the aircraft an additional 3 mins, 28 sec of full-throttle flight, but did not meet the static thrust to weight ratio if the aircraft was loaded to 18 lbs. The 13"x8" propeller superseded the power requirement, but decreased the endurance. Both propeller sets were purchased for the aircraft and were changed depending on the weight. The 13"x8" propellers were used when the aircraft was loaded to maximum gross weight. The 12"x8" propellers were used when aircraft weight fell below 17 lbs.

12.5 Endurance

A flight profile was created to approximate the aircraft's endurance. The motors would be accelerated to full power for 30 sec through takeoff roll and initial climb. Once a climb was established, the power would be decreased to 80% for 20 sec to climb to a 250 ft pattern altitude. At pattern altitude, the power would be decreased to 40% to maintain a 29 mph cruise. The power would be decreased to 15% during the aircraft's approach to landing, but this was not included in the endurance approximation to add a

factor of safety. Full-power endurance for the 12”x8” propellers would be 14 min, 4 sec. Full-power endurance would decrease for the 13”x8” props to 10 min, 36 sec. Following the flight profile would lead to a 45 min, 36 sec endurance with the 12”x8” propellers and a 28 min, 48 sec endurance with the 13”x8” propellers.

13 Landing Gear

A standard tricycle landing gear was constructed from a combination of aluminum, carbon fiber, and fiberglass to provide ample propeller clearance and strong support for grass runway takeoffs. The landing gear boasted a 26 inch wheel base and provided 3 inches of propeller clearance. The 5 inch diameter foam-filled rubber wheels were utilized to sustain the aircraft’s weight.

The main gear was fabricated from _” x 1/8” low-grade aluminum. To prevent the gear from buckling, a _” diameter carbon fiber tube was fiberglassed onto the aluminum. A steerable**,** dual strut nose gear constructed from _” diameter aluminum was used to complete the tricycle landing gear. A single Futaba 3000S servo was used to steer the nose gear.

14 Weights and Balance

14.1 Weight Distribution

The weight remained to be one of the largest restrictions during the design of the aircraft. After preliminary sizing, it was determined that the weight of the aircraft would

be 13 lbs. At this point a mass budget was created in order to maintain that ideal weight. The mass budget can be seen in Table 11. Each individual part and their approximate weights were listed.

Table 11: Design weight distribution

Part	Weight (lb)
Prop	0.1875
Motor	0.9875
Battery	1.24
Gear	0.375
Tire	0.1875
Wing	4
Fuselage	0.625
Tail Boom	0.25
Tail	0.5
Speed Control	0.09375
Receiver Battery	0.25
Wing Servo	0.25
Tail Servo	0.25
Pulley/cables	3
worm gear	0.75
Receiver	0.0625
Total	**13**

Throughout the continuation of the design the a few components increased in weight, exceeding the budget. Due to the constraints of time, money and technology, no other substitutes could be found (either purchased or fabricated) to reduce the weight. Following the finalization of all the parts, an updated mass budget was created. This new mass budget can be seen in Table 12 . The new weight of the aircraft was 18 lbs.

Table 12: Final weight distribution

Part	Weight (lb)
Prop/Motor	1.688
Battery	2.75
front gear	0.27
back gear	0.75
Wing	2.65
Fuselage	2.416
Speed Control	0.413
Receiver Battery	0.25
Wing Servo	0.25
pulleys	1.075
either pulleys	0.216
pods	1.225
cables	1.219
worm gear	1.525
Receiver	0.125
epoxy	0.563
spinners	0.75
Total	**18.135**

14.2 Center of Gravity Location

Through measurements it was determined that the center of gravity (CG) was located _" in front of the quarter chord. The landing gear was placed 1.25" (at a 9º angle) aft of the CG. The location of the landing gear relative to the CG guaranteed the aircraft was capable of rotation from a stability standpoint.

14.3 Effects of Adding Weight

By increasing the weight, the initial sizing requirements were altered. The lift coefficient, Reynolds number and wing loading were all constrained by the weight limit of 13 lbs. By increasing the weight the criteria needed to be analyzed to determine if it was within the design range.

Since the cruise lift coefficient was chosen to remain at the specified 0.61, the cruise velocity needed to be increased to a velocity of 40 ft/s. The wing loading was also increased from 0.81 to 1.17 and the new Reynolds number at cruise was increased to 320,000. Although these values increased, they are still within the design limits of a HALE aircraft.

15 Flight Testing

15.1 Summary of Flight Tests

Flight-testing of the aircraft was delayed until May 4, 2004 to complete construction and final bench testing of the aircraft systems. Four attempts were made at Christiansburg airfield in Christiansburg, VA to take off; all failed. In the first attempt, the aircraft accelerated approximately 75 ft down the runway to near rotation speed before the nose gear strut failed sending the aircraft into a ground roll. The nose gear was repaired and three more flights were attempted. In each case, the aircraft made it no more than 50 ft down the grass field before the main gear began to bend, causing the 5 inch tires to toe, pulling the aircraft uncontrollably to the left. The failure of the landing gear on takeoff roll did not permit the testing of the wing extension system in flight.

Figure 21 Bangle on first takeoff roll before nose strut failure

15.2 Landing Gear Failure

The failure of the landing gear was a result of inadequate structural strength for a grass field. The nose gear failed first due to shear. The aircraft hit a notch in the bumpy field creating a force opposing the direction of travel great enough to cause the nose gear to completely shear off. The nose gear was repaired on field using a _ inch brass sleeve that coupled the two broken ends of aluminum. The sleeve was epoxied in place and withheld the forces encountered in the remaining attempts.

The main gear retained its rigidity in the first flight attempt but failed by the second. The main gear was reinforced by carbon fiber that kept the gear from buckling. The gear withstood the loads and did not buckle, but rater failed near the axels. The double reinforced 1/8 inch aluminum bent at the base near the axles (Figure 22) causing the tires to toe inward. The toe created a large pull to the left, too great to be counteracted by rudder or steering the nose gear.

Figure 22: Main landing gear failure on second takeoff attempt

15.3 Aircraft Damage

The aircraft was severely damaged in the four attempts at flight. Aside from the failure of the main gear, damage occurred to the wing, motor mounts, and wing-extension system.

The left airfoil suffered failure across the trailing edge after the first flight attempt. Trailing edge stock as well as a number of ribs were severed. Both motor mounts were damaged after the first attempts as well. The right motor mount bent, but was easily corrected. The left motor mount not only bent, but cracked at the base rendering the motor inoperable.

The wing-extension system suffered catastrophic failure. The system was driven via a central pulley pinned into a _ inch aluminum drive shaft. The pulley was secured onto the shaft with a 1/8 inch pin. Multiple cycles with simulated aerodynamic loads in the lab resulted in the drive shaft failing at the pinning point due to shear. The pulley was re-pinned with a 5/64 inch pin forward of the failed drive shaft. The first roll transferred force through the left wing causing the drive shaft to fail again. The length of useable drive shaft is too short to re-pin the pulley. The entire motor and gearing system must be

extracted from the fuselage and drive shaft replaced with a higher grade aluminum or steel.

16 Conclusion

The mission of the 2003-2004 Morphing Wing Project was to design, build, and fly a remotely controlled HALE aircraft that aerodynamically scaled current HALE aircraft and exhibited a 300% wingspan change. The team successfully designed, bench tested, and taxi tested the aircraft. Though the aircraft was damaged due to landing gear failure in its flight-testing attempts, the semester was not a failure. The team designed, constructed, and demonstrated a HALE aircraft capable of extreme wingspan changes. The aircraft damage is repairable. The team hopes the following morphing wing design team will rebuild the crippled aircraft and demonstrate its morphing abilities in flight.

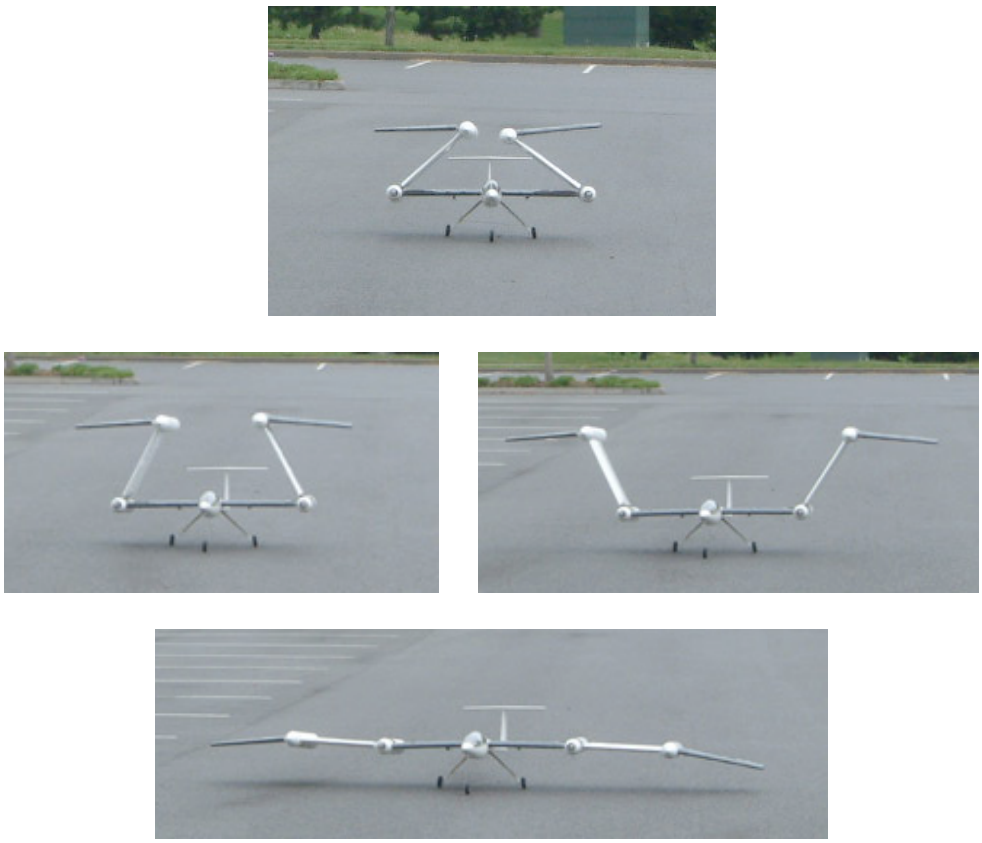

Figure 23: Wing extension series demonstrated in taxi-testing

Appendix 1: Cost

Virginia Tech was granted $70,000 towards the development of the morphing wing program, $10,000 of which was allocated to designing and constructing the HALE aircraft. Table 13 below itemizes the project costs. The project required half the funding it was granted.

Table 13: Itemized project costs

Product	Cost
2 TP7600 4S4P 14.8V Li-Po packs	602.37
Triton Li-Po charger	132.5
Vantec speed controller	95.99
Wing-extension motor	425
Props and Spinners (TH)	184.88
Loc/Precision Pods	121.25
Gears	89.45
Extensions, Monocoat, collars	141.9
MSC bearings	92.59
MSC drillrod for pins	15.53
1 Aveox F12S motor	341.45
1 F12S, SH-48 ESC, prop adapters	535.97
2 SH-96 electronic speed controllers	725
MSC drillrod for pins	30.8
Carbon Fiber tubs for spars	501.68
MSC 0.25" bore bearings	294.04
National Balsa for ribs	33.61
DG-505 aircraft for fuselage	524
Mis	378.82
Total HALE expenditure	5266.83

Appendix 2: Lessons Learned

Administration

- Have more than one member of the team machine shop certified. If none of the members are certified, look into a different design or another means of production.
- Since many ME's take the FE exam, account for a 2 week period around the time of the exam to allow for study time. During this time period work on the project will slow down drastically.
- Make a specified work time with a list of tasks to be accomplished at the beginning of each for each component to be worked on. This will limit overcrowding in the lab and will allow each member to take part in the construction phase.
- Have an AMA licensed pilot. If no pilot is available seek other sources (VT Design Build Fly Team).

Design/Building

- Ensure that the landing gear is stable and robust enough to take off on either asphalt or medium length turf, depending on the location of the flight test (Salem or Christiansburg)

- Incorporate outside sources (professors from other departments, companies, model aircraft enthusiasts, etc.). They are valuable resources and are normally willing to lend a hand.
- Before attaching components permanently, make sure that all parts fit correctly
- Make sure that any special techniques or materials that are needed to complete construction are known well in advance.
- Given more time, the team would have liked to increase the effectiveness of the elevators. The elevators could have been increased both in the spanwise and chordwise directions to provide more control authority and increase the horizontal tail area. To prevent the aircraft from being too sensitive on takeoff and landing, the radio should have been programmed with dual rates and exterpolation to control the amount of elevator deflection for the two main flight configurations.

Testing

- Choose a proper airfield that can accommodate the needs of the aircraft (if the landing gear was designed for an asphalt runway, do not takeoff of a turf runway).
- Make sure the prop-line is clear of any persons before starting the engine.
- Program a failsafe into the controller in case of a loss of signal. Most controllers have the capability having a fail-safe programmed into it. If the signal to the aircraft (from the controller to the receiver) is lost, then the aircraft will automatically cut off the engine and pitch the aircraft into the ground.

- If using Lithium Polymer battery cells, be aware of the possible dangers associated with them. For more information contact the AMA or go to their website: http://www.modelaircraft.org/templates/ama/.

Tornado

The team used Tornado, a vortex lattice code, for a large portion of the stability analysis. However, there are some idiosyncrasies with Tornado that users should be familiar with. The team validated Tornado with data for a Cessna 172. The code showed relatively good correlation, except for some lateral-directional derivatives (mainly $C_{n_}$ and $C_{l_}$) that were calculated as unstable by Tornado. Further exploration of the code determined why. By inputting a simple rectangular wing into Tornado and adding a small amount of dihedral, $C_{n_}$ became increasingly negative. This is opposite of conventional stability and control intuition; therefore, the sign of $C_{n_}$ must be switched in the Tornado output. The same test case also determined that $C_{l_}$ was the incorrect sign. Therefore, it is important to remember when using Tornado that the signs of $C_{n_}$ and $C_{l_}$ are incorrect. All other signs should be correct.

Appendix 3: References

Lednicer, David. "The Incomplete Guide to Airfoil Usage." Available:

http://www.aae.uiuc.edu/m-selig/ads/aircraft.html.

Melin, Thomas. Tornado: A Vortex Lattice MATLAB Implementation for Linear Aerodynamic Wing Applications. Available:

http://www.flyg.kth.se/divisions/aero/software/tornado/.

Kay, Jacob, W.H. Mason, W. Durham, F. Lutze and A. Benoliel, "Control Power Issues in Conceptual Design: Critical Conditions, Estimation Methodology, Spreadsheet Assessment, Trim and Bibliography," VPI-Aero-200, November 1993.

Raymer, Daniel P. Aircraft Design: A Conceptual Approach, 3rd Edition. AIAA Education Series: 1999.

NASA, Dryden Flight Research Center

http://www.dfrc.nasa.gov

Federation of American Scientists, "Intelligence Resource Program"

http://www.fas.org/irp/program/collect/uav.htm